Dendritic Cell Targeting mRNA Lipopolyplexes Combine Strong Antitumor T-Cell Immunity with Improved Inflammatory Safety

Kevin van Der Jeught, Stefaan de Koker, Lukasz Bialkowski, Carlo Heirman, Patrick Tjok Joe, Federico Perche, Sarah Maenhout, Sanne Bevers, Katrijn Broos, Kim Deswarte, et al.

Dendritic Cell Targeting mRNA Lipopolyplexes Combine Strong Antitumor T-Cell Immunity with Improved Inflammatory Safety

Kevin Van der Jeught[†,§], Stefaan De Koker[‡,§], Lukasz Bialkowski[†], Carlo Heirman[†], Patrick Tjok Joe[†], Federico Perche[‖], Sarah Maenhout[‡], Sanne Bevers[‡], Katrijn Broos[†], Kim Deswarte[⊥], Virginie Malard[‖], Hamida Hammad[⊥], Patrick Baril[‖], Thierry Benvegnu[▲], Paul-Alain Jaffrès[■], Sander A.A. Kooijmans[¶], Raymond Schiffelers[¶], Stefan Lienenklaus[⊤], Patrick Midoux[‖], Chantal Pichon[‖, *, #], Karine Breckpot[†, *, #], Kris Thielemans[†, *, #]

[†] Laboratory of Molecular and Cellular Therapy, Department of Biomedical Sciences, Vrije Universiteit Brussel (VUB), Brussels, Belgium

[‡] eTheRNA Immunotherapies NV, Niel, Belgium

[‖] Centre de Biophysique Moléculaire, CNRS UPR 4301, University and Inserm, Orléans, France

[⊥] VIB Inflammation Research Center, UGent, Ghent, Belgium

[▲] Ecole Nationale Supérieure de Chimie de Rennes, CNRS UMR6226, Rennes, France

[■] CEMA, CNRS UMR 6521, SFR148 ScInBioS, Université de Brest, Brest, France

[¶] University Medical Center Utrecht, Universiteit Utrecht, Utrecht, Netherlands

[⊤] Hannover Medical School, Hannover, Germany

[§] Contributed equally to this work

[#] Shared senior authorship

ABSTRACT:

In vitro transcribed (IVT) mRNA constitutes a versatile platform to encode antigens and to evoke CD8 T-cell responses. Systemic delivery of mRNA packaged into cationic liposomes (lipoplexes) has proven particularly powerful in achieving effective antitumor immunity in animal models. Yet, T-cell responses to mRNA lipoplexes critically depend on the induction of type I interferons (IFN), potent pro-inflammatory cytokines, which inflict dose limiting toxicities. Here, we explored an advanced hybrid lipid polymer shell mRNA nanoparticle (lipopolyplex) endowed with a tri-mannose sugar tree as alternative delivery vehicle for systemic mRNA vaccination. Alike mRNA lipoplexes, mRNA lipopolyplexes were extremely effective in conferring antitumor T-cell immunity upon systemic administration. Conversely to mRNA lipoplexes, mRNA lipopolyplexes did not rely on type I IFN for effective T-cell immunity. This differential mode of action of mRNA lipopolyplexes enabled the incorporation of N1 methyl pseudo-uridine nucleoside modified mRNA to reduce inflammatory responses without hampering T-cell immunity. This feature was attributed to mRNA lipopolyplexes, as the incorporation of thus modified mRNA into lipoplexes resulted in strongly weakened T-cell immunity. Taken together, we have identified lipopolyplexes containing N1 methyl pseudo-uridine nucleoside modified mRNA as potent yet low inflammatory alternatives to the mRNA lipoplexes currently explored in early phase clinical trials.

KEYWORDS: mRNA, lipopolyplexes, type I interferon, cancer therapy, T cell, modified nucleosides

In vitro transcribed (IVT) messenger RNA (mRNA) constitutes a versatile platform to deliver antigenic information to the immune system. Systemic administration of mRNA packaged into **L**ipid based m**R**NA nanocomplexes (LR) has emerged as a particularly powerful approach to yield potent antitumor T-cell responses.[1-3] Inevitably, systemic administration of mRNA encapsulated into nanoparticles comes at the expense of an increased risk of adverse events. Toxicity to systemic administration of mRNA nanoparticles is multifaced but closely linked to the secretion of inflammatory cytokines.[4] These inflammatory responses are associated with liver damage and hematological toxicities and should hence be minimized to increase safety.[5,6] To avoid these inflammatory responses, the RNA field has designed several mRNA modifications that strongly reduce RNA sensing by innate sensors.[7-9] Although avoidance of innate activation is vital when using mRNA in the context of protein replacement therapy, a certain level of innate immune activation needs to be maintained to evoke T-cell immunity in the context of mRNA vaccination. Identification of an mRNA nanoparticle format that combines excellent immunogenicity with sufficient (inflammatory) safety thereby represents a major challenge to enable safe application of systemic mRNA vaccines.

LR elicit potent cytokine responses reminiscent of systemic viral infections upon systemic administration that can be a cause of adverse effects, ranging from mild flu-like symptoms to liver toxicities and auto-immune pathologies.[10-12] Hybrid **L**ipidshell **P**olymer core m**R**NA nanoparticles (LPR) might represent valuable alternatives to LR as they combine improved colloidal stability with reduced cytotoxicity.[13,14] Moreover, the physicochemical properties of LPR are likely to result in a differential interaction of the delivered mRNA with innate RNA sensors, which in turn might alter the immunogenicity and safety profile of LPR relative to LR. In this study, we thereby addressed the T-cell responses and inflammatory responses to an advanced LPR platform comprising a lipid shell endowed with Mannose Receptor targeting moieties.[15,16] LPR exhibited excellent hemocompatibility and largely restricted mRNA expression to splenic antigen presenting cells upon systemic administration. Immunization with LPR instigated potent T-cell immunity and showed superior effectiveness in controlling tumor growth compared to

intravenous immunization with antigen mRNA electroporated dendritic cells (DCs) and LR. Early innate responses to LPR were characterized by a type I IFN signature in the spleen. Nonetheless, conversely to LR, LPR did not depend on these type I IFN responses to generate cytolytic effectors. This striking behavior of LPR enabled the generation of a less pro-inflammatory yet equally potent systemic LPR vaccine by usage of N1-methylpseudo-uridine nucleoside modified mRNA (see **Graphical Table of Contents**).

RESULTS AND DISCUSSION:

Synthesis and characterization of Tri-Mannosylated LPR

LPR nanoparticles were produced by a well-established two-step approach, comprising first the complexation of mRNA to a cationic polypeptide PEG-HpK at mRNA/polymer at weight ratio of 1/3 and then a subsequent mixing of the generated mRNA polyplexes with liposomes at mRNA/lipid weight ratio of 1/2.[17] The previously described polyethylene glycol (PEG)ylated derivative of histidylated polylysine was used to complex the mRNA into polyplexes. Liposomes were derived from those reported by Perche *et al*. yet the mono-mannose bearing lipid was replaced by a tri-mannose bearing diether lipid as this was demonstrated to further increase the selectivity of Mannose Receptor targeting *in vitro.*[15,16] The LPR generation and characteristics are shown in **Figure 1A-B**. The complexation of mRNA was confirmed by the absence of mRNA migration in an agarose gel electrophoretic mobility shift assay (**Figure 1C**). Moreover, mRNA was stable as evidenced by the absence of degradation when LPR was mixed with Fetal Clone I serum in contrast to 'naked' mRNA (**Figure 1C**). To assess mRNA integrity upon LPR incorporation, we extracted the mRNA from LPR using TRizol extraction agent and performed capillary gel electrophoresis (Agilent). As can be appreciated from **Figure 1D**, mRNA integrity was not affected upon LPR generation. The morphology of LPR was assessed by Transmission electron microscopy (TEM). Liposomes exhibited a spherical shape with a laminar lipid bilayer structure (**Figure 1E**). Tri-mannosylated LPR displayed the core morphology of mRNA/PEG-HpK polyplexes, which appeared surrounded by a laminar lipid bilayer structure of liposomes (**Figure 1F-G**). How polyplexes become encapsulated into

liposomes is not yet fully understood. The charge of mRNA polyplex is close to neutrality due to the presence of PEG on the polymer, this prevents strong repulsion between cationic liposomes and polyplexes favoring their interaction and encapsulation of polyplexes into the liposomes. The interaction may be also favored by (i) local high concentration of PEG favoring lipid mixing and/or bilayer destabilization and (ii) interaction between imidazole groups of the polyplex and those of the polar heads of lipids. Altogether, those interactions could favor polyplexes encapsulation.

The association of mRNA, lipids and polymer was addressed by flow cytometry through usage of fluorescein-labelled liposomes, Cy3-labelled mRNA and Cy5-labelled polymer. The results indicated that the liposomes, the polymer and the mRNA were associated in a same particle. Based on the side and forward scatters of polyplexes, liposomes and LPR, no free polyplexes were detected in the LPR solution indicating that all polyplexes were encapsulated inside liposomes (**Figure S1**).

Intravenous LPR administration targets and activates splenic antigen presenting cells

The spleen constitutes the lymphoid organ where T-cell immunity against blood-borne antigens is initiated and thereby represents the major target of systemic mRNA vaccines. The functional bio-distribution of mRNA was assessed through incorporation of Firefly Luciferase (Fluc) encoding mRNA into LPR and full body bioluminescence imaging (BLI). A rapid and sustained Fluc expression was observed in the spleen, whereas no significant expression was detectable in other body parts. These data were confirmed by organ isolation, which showed an exclusive splenic BLI signal (**Figure 2A-B**). Of note, LPR were previously reported to be also delivered in other organs and notably in the liver.[15] Nevertheless, no luciferase expression was observed in the liver. Splenic expression was strongly diminished in transgenic CD11c-diphtheria toxin (DT) receptor mice treated with DT prior to Fluc mRNA LPR administration (**Figure 2C**), suggesting mRNA expression predominantly occurs in DCs. To further delineate the location of the mRNA uptake we incorporated Cy5-labeled mRNA into LPR. Sections obtained from spleens dissected four hours post injection were stained for CD3 and B220 to respectively visualize T cells and B cells present in the white pulp. Large

numbers of Cy5-labeled LPRs accumulated in the area surrounding the white pulp, which corresponds to the marginal zone sinuses of the spleen (**Figure S2**). To characterize more specifically the cell types that express LPR delivered mRNA, we injected *ROSA26-loxP-Stop-loxP RFP* transgenic mice with LPR that contain CRE Recombinase mRNA.[18] In these mice, cells expressing CRE will remove the floxed stop codon enabling Red Fluorescent Protein expression to unfold. Spleen sections stained for CD11c and MOMA-1 revealed RFP expression in CD11c DCs, yet also in MOMA-1 macrophages (**Figure 2D**). When LR were modified with tri-mannose, a BLI signal was also detected in the spleen, but the BLI signal in LPR injected mice was higher than in LR injected mice (**Figure S3**). The higher BLI signal suggested either a better transfection efficiency of DC with LPR than with LR or a better delivery of LPR in the spleen notably in splenic DCs.

DC maturation constitutes an essential prerequisite for efficient T-cell priming and effector/memory T-cell differentiation. We thereby determined the maturation status of CD8a DCs and of CD11b DCs - the two major conventional DC populations present in the spleen.[19] An overview of the gating strategy applied to identify splenic DC subsets is given in **Figure S4**. In response to systemic LPR administration, CD8a DCs - the cross-presenting DC subset generally considered vital for initiation of CD8 T-cell immunity - exhibited a pronounced upregulation of MHC class II, CD86 and CD40. [20] CD86 and CD40 were also upregulated on the CD11b DC subset, albeit to a lesser extent (**Figure 2E**). Taken together, these data demonstrate that systemic administration of LPR not only targets mRNA expression to the relevant antigen presenting cells of the spleen, but also properly activates them to subsequently prime T cells.

Systemic administration of LPR instigates superior T-cell immunity compared to LR

Next, we determined the capacity of systemic LPR vaccination to stimulate CD8 T-cell immune responses against the model antigen ovalbumin (OVA) and against the Human Papillomavirus 16 (HPV16) oncoprotein E7. Cytolytic T-cell responses were quantified after single LPR administration using a well-established *in vivo* killing assay.[21] LPR immunization induced strong target cell lysis against both antigens. Addition of TriMix

mRNA - a mixture of mRNAs encoding the immune-stimulatory proteins CD40L, CD70 and caTLR4 – to the antigen encoding mRNA further enforced the evoked cytolytic T-cell responses (**Figure 3A**).[22,23] These responses increased in a dose dependent fashion, evidenced by the increased percentages of OVA-specific CD8 T cells and by the elevated numbers of IFN-γ secreting OVA-specific T cells at the higher dose (**Figure S5A-B**). Repeated immunizations with OVA/TriMix mRNA LPR profoundly expanded the circulating antigen-specific T-cell pool, resulting in an impressive percentage of OVA-specific CD8 T cells (51% +/- 10%) 19 days after the initiation of immunization (**Figure 3B**). These strong OVA-specific T-cell responses were sustained over a long period of time and slowly decreased, as over 20% of all peripheral CD8 T cells remained antigen-specific one month after the third immunization. Subsequent boosting resulted in a rapid recall response, indicative of memory conversion (**Figure 3B**). After the final boost, a high fraction of splenic antigen-specific CD8 T cells produced IFN-γ (38%+/-4%) and a significant amount of antigen-specific T cells co-produced IFN-γ and TNF-α (6%+/-1%), indicative of a polyfunctional effector phenotype, which has been associated with improved T cell functionallity (**Figure 3C**).[24] Compared to LR with the same lipid composition, mice bearing TC-1 tumor cells injected with LPR encoding E7 demonstrated the advantage for the addition of the PEG-HpK on the Tri-mannosylated liposomes (**Figure S6**). The results were in line with those reported by Mockey *et al.* showing that LR was not an efficient formulation to induce a specific immune response upon intravenous injection.[25] In addition, the advantage of the Tri-mannosylated liposomes over non-mannosylated liposomes is also shown, and in line with results previously reported.[15] Thus, even with Tri-Man targeting DCs, the efficiency of LR was still lower than with LPR.

Systemic LPR administration elicits profound antitumor immunity

The therapeutic benefit of systemic LPR immunization was assessed in the aggressive TC-1 tumor model, which expresses the HPV16 oncoprotein E7. Therapeutic vaccination consisted of three IV immunizations with E7/TriMix mRNA LPR. Antitumor efficacy was benchmarked against immunization with LR (**Figure 4A-B**) and *ex vivo* generated DCs electroporated with E7/TriMix mRNA (**Figure S7A-C**). TriMix/antigen

mRNA electroporated DCs were selected as benchmark as this approach was demonstrated to be sufficiently powerful to yield clinical benefit in melanoma patients in a phase II study.[26] Systemic LPR treatment dramatically improved the median survival time of TC-1 inoculated mice and was even superior in controlling tumor growth in comparison to treatment with LR and electroporated DCs, respectively. As a consequence, these data highlight the capacity of LPR to yield effective antitumor immunity.

LPR induced type I IFN are dispensable for cytolytic T-cell differentiation

mRNA complexed to lipid carriers (LR) instigates vigorous type I interferon (IFN) responses upon *in vivo* administration. Alike the LR described previously, LPR evoked transiently elevated IFN-α titers in blood (**Figure 5A**).[1,2] To pinpoint the anatomical location of type I IFN induction a transgenic IFN-β reporter mouse strain was used.[27] In this mice strain, a Luciferase encoding gene sequence was placed under control of the IFN-β promoter. Full body imaging revealed a strong bioluminescence signal confined to the spleen of LPR injected mice, whereas no IFN-β promoter activation was observed in non-lymphoid organs typically associated with nanoparticle accumulation such as liver and lungs (**Figure 5B**). This selective type I IFN induction can be considered highly beneficial, as the presence of type I IFN in lymphoid tissues is likely to maximize T cell immunity, whereas absence of type I IFN induction in vital organs such as lungs and liver should minimize adverse effects.

NanoString transcriptome analysis further confirmed the existence of a strong antiviral-like type I IFN signature in the spleen (**Figure 5C**), with upregulation of mRNAs encoding IFN-β, IFN-α isoforms and downstream Interferon Stimulated Genes (ISGs). Transcripts encoding the intracellular RNA sensors RIG-I (ddx58) and MDA-5 (Ifih1) were upregulated alongside transcripts that encode the 2'-5'-Oligoadenylate Synthetases (OAS) 2 and 3. OAS2 and OAS3 are activated by double stranded (ds) RNA and induce RNA cleavage by activation of RNAseL.[28] Transcripts for endosomal TLRs recognizing viral RNAs (TLR3, TLR7) were increased, whereas transcript levels for TLR recognizing bacterial ligands (TLR4 and TLR5) remained unaffected or were even slightly downregulated. In addition to these typical antiviral mediators, spleens of

LPR injected mice upregulated mRNA encoding IL-12, the most potent polarizing cytokine driving Th1 and cytolytic T-cell responses. Transcript levels of IL-6 and CCL-2 were moderately elevated, whereas those of IL-1α, IL-1β and TNF-α only displayed marginal increases. No inductions of the canonical Th2 (IL-4) or Th17 (IL-17) cytokines were observed, whereas mRNA levels of the Th1 oriented cytokines IFN-γ and CXCL-10 were increased.

Type I IFN have been attributed vital roles in instigating cytolytic effectors upon systemic immunization with mRNA lipoplexes (LR).[1,2] To decipher whether the induction of cytolytic effectors also relies on type I IFN upon systemic LPR immunization, we compared cytolytic T-cell responses between wild type mice and mice lacking the common IFNα/β receptor (IFNAR). IFNAR deficiency did not hamper cytolytic activity upon LPR vaccination (**Figure 5D-E**). This striking type I IFN independent behavior of LPRs was not caused by the immune-stimulatory functions of TriMix mRNA as LPR containing antigen mRNA without TriMix mRNA displayed an identical type I IFN independent behavior (**Figure 5E**). Conversely, mRNA lipoplexes (LRs) with identical lipid composition yet lacking the polymeric core did heavily depend on type I IFN to instigate cytolytic T-cell responses even in the presence of TriMix mRNA (**Figure 5F**). Together, these data demonstrate that type I IFN are dispensable to induce cytolytic T cells upon LPR immunization.

N1mψ modified mRNA reduces inflammatory responses to systemic LPR immunization

Incorporation of naturally occurring nucleoside modifications can reduce innate sensing of IVT mRNA and thereby dampen inflammatory cytokine responses.[7, 29-34] Given the type I IFN independency of systemic LPR immunization, we speculated that the combination of nucleoside modified mRNA with the LPR platform might enable high therapeutic efficacy alongside diminished inflammatory responses. Pseudo-uridine has been the most widely explored nucleoside modification to reduce innate responses to mRNA, yet pseudo-uridine modified mRNA failed to reduce inflammatory responses to systemic mRNA delivery using a lipid based nanoparticle (LNP) platform.[35] N1-methyl-pseudouridine (N1mψ) might represent a nucleoside modification with superior

capacities to reduce innate RNA recognition and to increase the translational capacity of mRNA.[9, 36-39]

First, we addressed the impact of N1mψ nucleoside modified mRNA on serum titers of inflammatory cytokines after systemic LPR administration. Cytokine heatmaps obtained at respectively 2 hours and 6 hours post injection revealed a general reduction in inflammatory responses to LPR containing N1mψ nucleoside modified mRNA (**Figure 6A-B** and **Figure S8A-D**). Unmodified mRNA LPR instigated strong increases in serum titers of IFN-α, IL-6, CCL-2 (MCP-1), CXCL-10 (IP-10), mirroring the increased expression levels we detected for these cytokines in the spleen. IL-12 and TNF-α were moderately elevated, whereas levels of IL-1α and IL-1β were only slightly augmented compared to untreated mice. Use of N1mψ nucleoside modified mRNA resulted in a reduced pro-inflammatory cytokine profile in blood of LPR treated mice, with prominently reduced titers of IFN-α and of IL-6. Levels of IL-12 and CXCL-10 were also significantly reduced, albeit to a lesser extent. CCL-2 was significantly reduced at two hours post injection but not at 6 hours post injection (**Figure 6A** and **Figure S8D**). IL-1α, IL-1β were only marginally upregulated irrespective of the mRNA format (**Figure 6A** and **Figure S8A-B**). Bioluminescence imaging of IFN-β reporter mice confirmed the reduced IFN-β promoter activation upon injection of N1mψ nucleoside modified mRNA LPR (**Figure 6C**).

We next analyzed the impact of N1mψ nucleoside modified mRNA on the biodistribution and intensity of mRNA expression upon systemic LPR administration. LPR containing N1mψ nucleoside modified Fluc mRNA retained the spleen-centered expression pattern of unmodified mRNA (**Figure S9A**) and induced elevated levels of Fluc expression compared to LPR containing unmodified mRNA (**Figure S9B**).

N1mψ modified mRNA does not hamper antitumor T-cell immunity to LPR

To address how the combination of elevated antigen expression levels with reduced inflammatory responses upon use of N1mψ nucleoside modified mRNA impacts the magnitude of the LPR instigated T-cell responses, we quantified the percentages of circulating antigen-specific T cells and their IFN-γ secretion upon restimulation. N1mψ

nucleoside modified mRNA did not interfere with the initial priming and expansion of antigen-specific T cells. Instead, after the third immunization, mice immunized with N1mψ nucleoside modified mRNA LPR even displayed elevated percentages of antigen-specific CD8 T cells (**Figure 7A-C**). The fraction of OVA specific CD8 T cells that rapidly responded with IFN-γ secretion upon *in vitro* peptide restimulation was however reduced from 60% (unmodified mRNA) to approximately 40% in the modified mRNA group (**Figure 7D**). These data support a model in which usage of modified mRNA in LPR context supports elevated T cell proliferation - by enhancing antigen expression and presentation - yet results in relatively lower percentages of T cells displaying immediate effector function, which most likely is a consequence of reduced inflammatory cytokines titers that impose effector function. Combined, these data fit into the hypothesis that high TCR stimulation combined with low to moderate levels of cytokines promote central memory T cell responses, whereas TCR stimulation in the context of high inflammation rather promotes effector/effector memory differentiation.

The functionality of the elicited T cells was assessed by comparison of antigen-specific cytolytic activity after immunization with of OVA/TriMix unmodified mRNA LPR or with OVA/TriMix N1mψ nucleoside modified mRNA LPR (**Figure 7E-F**). Cytolytic effector T-cell responses were not dampened by N1mψ nucleoside modified mRNA. In line with our observations in Ifnar$^{-/-}$ mice, this striking feature was intrinsic to LPR, as LR (identical lipid composition yet lacking the polymeric LPR core) largely lost their capacity to elicit cytolytic effectors upon incorporation of N1mψ nucleoside modified mRNA (**Figure 7E**). To assess whether these features are specific to the tri-mannosylated LPR system applied in this study or represent a common property of LPR, we designed an LPR system with a lipid shell composed of RNAiMAX.[1] RNAiMAX based LPR and LR behaved identical to the tri-mannosylated LPR/LR system: equal cytolytic activity when N1mψ nucleoside modified mRNA is applied in an LPR context, whilst a reduction in cytolytic activity upon N1mψ nucleoside modified mRNA delivery in an LR context (**Figure 7F**). The better quality of the immune response including the amount of antigen-specific CD8 T cells (**Figure 7G**) induced with LPR as compared to LR might be due to supramolecular organization of mRNA with the polymer and liposomes in LPR and of

mRNA with liposomes in LR, which likely makes the difference. In the LPR formulation, the mRNA is condensed with the polymer and then encapsulated in a liposome. In contrast, mRNA is sandwiched between lipid layers in LR. The targeting to DCs of LR and LPR by mannose moieties *via* the mannose receptor would not be different. However, the presence of the mRNA-condensing polymer would modify the release and/or intracellular trafficking of mRNA and therefore the sensing by pattern recognition receptors as those involved in IFN type I activation. We showed that similar effect but in a lower extent was obtained with RNAiMAX-based LR and LPR. Therefore, the mRNA complexation with the cationic polymer would be rather responsible than the nature of liposomes.

The antitumor capacities of systemic immunization with N1mψ nucleoside modified mRNA LPR and unmodified mRNA LPR were compared in the subcutaneous TC-1 (**Figure 7H-J**) and B16-OVA tumor models (**Figure 7J**). The growth curve shows the lack of growth control for LR with N1mψ nucleoside modified mRNA, as opposed to the LPR treated mice where no significant differences were observed between the two treatment groups. Similar observations were obtained in the highly aggressive subcutaneous B16-OVA model, with both treatment modalities being equally potent in stalling tumor growth (**Figure 7J**). Taken together, these data demonstrate LPR can be combined with N1mψ nucleoside modified mRNA to improve inflammatory safety upon systemic administration without hampering the functionality and antitumor efficacy of the evoked T cell response.

Incorporation of N1mψ nucleoside modified mRNA reduces LPR evoked type I IFN on human PBMCs

Finally, we aimed to assess the translational potential of using N1mψ modified nucleoside mRNA LPR by assessing hemocompatibility, transfection efficiency and cytokine responses on human peripheral blood mononuclear cells (PBMCs). The hemocompatibility of LPR was addressed on human blood according to the guidelines of the US Nanotechnology Characterization Laboratory (NCL). LPR were evaluated at mRNA plasma-concentrations corresponding to intravenous injection of respectively 1250 µg (223 ng/ml), 250 µg (44.6 ng/ml) or 50 µg of mRNA (8.9 ng/ml). At none of the

assayed doses, LPR induced significant complement activation - as determined by Western Blot quantification of C3a cleavage (**Figure 8A-B**). Hemolysis was determined through measurement of hemoglobin release on Li-heparin anticoagulated blood from two different healthy donors. None of the LPR incubated samples showed significant hemolysis according the NCL criteria (**Figure 8C**). Finally, platelet aggregation was quantified on pooled platelet rich plasma (PRP) obtained from four healthy donors. At the evaluated doses, LPR did not evoke significant platelet aggregation (**Figure 8D**). To assess whether LPR can transfect human antigen presenting cells, we incubated monocyte derived DCs from healthy donors with LPR containing eGFP mRNA. As can be appreciated from **Figures S10A-B**, LPR were capable of mediating DC transfection without severe impact on cell viability. Finally, we addressed to which extent the reduction in inflammatory cytokines observed in mice upon usage of N1mψ modified mRNA could be extended to human PBMCs. Alike our findings in mice, incorporation of N1mψ nucleoside modified mRNA strongly reduced IFN-α and IFN-β titers produced by human PBMCs upon incubation with LPR, suggesting that our data can be translated to the human setting (**Figure 8E-F**).

CONCLUSIONS:

In conclusion, we have demonstrated that systemic immunization with LPR comprising histidinylated polylysine and Tri-Mannosylated and imidazoylated liposomes elicits strong cytolytic T-cell responses that confer high antitumor efficacy. In contrast to LR made with same liposomes, cytolytic T-cell responses to LPR immunization did not require type I IFN responses. Incorporation of N1mψ modified mRNA increased mRNA expression levels and reduced inflammatory responses, without hampering T-cell mediated antitumor efficacy. LPR displayed excellent hemocompatibility on human blood and incorporation of N1mψ modified mRNA into LPR dramatically reduced type I IFN secretion upon incubation with human PBMCs. Taken together, by combining excellent immunogenicity with improved inflammatory safety, those LPR constitute an interesting alternative to the current developed LR.

MATERIALS AND METHODS:

Mice. 6-12 week old female C57BL/6 mice were purchased from Charles River (France). Ifnar$^{-/-}$ were kindly provided by C. Libert (Ghent University, Belgium). CD11c-DTR mice and *ROSA26-loxP-Stop-loxP RFP* transgenic mice were kindly provided by B. Lambrecht (Ghent University, Belgium). IFN-β reporter mice were provided by S. Lienenklaus (Hannover Medical School). All mice were housed in individually ventilated cages and handled according to the regulations of the Animal Ethics and Animal Care Committee of the Vrije Universiteit Brussel.

Cell line and reagents. The TC-1 cell line was obtained from T.C. Wu (Johns Hopkins Medical Institution, Baltimore, Maryland, USA). The expression of the viral proteins HPV16-E6 and HPV16-E7 was confirmed by RT-PCR. The HEK 293T cells and the melanoma B16-OVA cells were obtained and cultured as recommended by the American Type Culture Collection.

The HPV16 E7-derived peptide RAHYNIVTF and the OVA-derived peptide SIINFEKL were purchased from Eurogentec (Belgium).

mRNA production. mRNA encoding caTLR4, mouse CD70, mouse CD40L, Fluc, eGFP, HPV16 E7/DCLamp, tNGFR and OVA was used throughout the study. The mRNA was transcribed from the following previously described plasmids pEtheRNA-v2-TLR4, pEtheRNA-v2-moCD70, pEtheRNA-v2-moCD40L, pEtheRNA-v2-Fluc, pEtherna-v2-eGFP, pEtheRNA-v2-sig-E7/16-DCLco, pGEM-tNGFR and pGEM-li80tOVA, respectively.[1,40,41] The mRNA transcription and quality control were performed as previously described.[40]

Lipids, Liposomes and polymer. The trimannosyl diether lipid (TriMan-Lip), *O*,*O*-dioleyl-*N*-[3*N*-(*N*-methylimidazolium iodide) propylene] phosphoramidate (Lip1) and *O*,*O*-dioleyl-*N*-histamine phosphoramidate (Lip2) were synthesized as described.[16,42] TriManlip100 liposomes were prepared at 5.4 mM by mixing in ethanol Lip1, Lip2 and TriMan-Lip in the percentage of 47.5%, 47.5% and 5%, respectively. Solution was then evaporated until formation of a film. The film was hydrated for 12 h at 4°C in 1 mL of 10 mM RNase free HEPES buffer, pH 7.4, vortexed and then the suspension was

sonicated for 15 min at 37 kHz using a Bioblock ultrasonic bath (Bioblock Scientific, Illkirch, France). Liposomes were dialyzed (Dialysis Tubing Cellulose membrane; MWCO: 12.4 kDa; size: 33 x 21 mm, Sigma) at 4°C for 6 hours and then overnight against 500 mL 10 mM RNase free HEPES buffer, pH 7.4. The lipid concentration was determined with Nile Red. The amount of mannosylated lipid per liposome was determined using the colorimetric resorcinol/sulfuric assay.[43] PEGylated and histidinylated polylysine (PEG-HpK; average Mw of 75.4 kDa) was poly-L-lysine of degree of polymerization substituted at 45% with histidine residues and one mPEG molecule of 5 kDa prepared as described.[25,44]

LPR preparation. LPRs were prepared as previously described.[15] In brief, mRNA was first complexed with PEG-HpK by vortex at an mRNA/PEG-HpK weight ratio of 1/3. The resulting polyplexes were incubated with TriManlip100 liposomes or RNAiMAX liposomes at an mRNA/liposome ratio of 1/2. LR were formed by mixing mRNA with TriManlip100 liposomes or RNAiMAX liposomes at an mRNA/liposome ratio of 1/2.

Electrophoretic mobility shift assay and particle characterization. The size and zetapotential of LPR was measuredusing SZ-100 Analyser (Horiba Scientific, les Ulis, France), the electrophoretic mobility shift assay were performed as described earlier.[1]

Transmission electron Microscopy (TEM). The sample solutions were deposited on carbon grid (for 10 min) and then rinsed three times with distilled water. The samples were then stained with uranyl acetate for 30 sec. Finally, the grids were washed twice with distilled water prior to air-drying. The samples were observed under TEM (CM20 Philips, FEI company, Oregon, USA) equipped with LaB6 filament and operating at 160 kV.

Immunization of mice. Mice were immunized at the indicated dose and mRNA composition intravenously formed as LPR in a final volume of 250 µl 10 mM Hepes and 5 % glucose (pH 7.4).

***In vivo* bioluminescence imaging.** *In vivo* bioluminescence imaging was conducted on the Photoimager Optima (Biospacelab, France) using the Photo Acquisition software

Version 3.4 (Biospacelab, France) and the analysis M3 Vision Software 1.0.7.1178 (Biospacelab, France) as previously described.[45]

***In vivo* killing assay.** The assay was performed as previously described.[1]

Cytokine secretion by peripheral blood mononuclear cells (PBMCs). PBMCs were isolated from whole blood and cultured according to procedure ITA-10 described by the Nanoparticle Characterization Laboratory (NCL) of the National Cancer Institute (http://ncl.cancer.gov). In brief, blood was withdrawn from healthy volunteers and anticoagulated with lithium heparin. Withdrawal of blood samples was approved by the University Medical Center Utrecht (UMCU) Ethics Committee. Cells were resuspended in culture medium (RPMI 1640; ThermoFisher Scientific) containing 10% fetal bovine serum (FBS) and 100 U/mL penicillin and streptomycin) at a final concentration of 1.3 x 10^6 cells/mL. 800 µL of cell suspension was seeded in 24-well plates and mixed with 200 µL of nanoparticle solution in duplicate in PBS. Cells were cultured at 37°C and 5% CO_2 for 24 hours, after which supernatants were collected. Cytokine release profiles were determined using an in-house developed and validated (ISO9001 certified) multiplex immunoassay (Laboratory of Translational Immunology, UMCU) based on Luminex technology (xMAP, Luminex, Austin, USA). Data was acquired with a Bio-Rad FlexMAP3D system (Bio-Rad laboratories, Hercules, USA) with xPONENT software version 4.2 (Luminex).

NanoString analysis. Total RNA was isolated from the spleen of mice using the SV Total RNA Isolation System (Promega, Madison, USA). The Samples were then analyzed with the PanCancer Immune Profiling Panel according to the manufacturer's instructions and run on the nCounter SPRINT Profiler. The data were analyzed using the nSolver software.

Platelet aggregometry. Platelet aggregations were performed according to procedure ITA-2.2 described by the NCL, with minor modifications. In brief, blood was withdrawn from healthy volunteers and anticoagulated with 3.2% w/v trisodium citrate. Whole blood was centrifuged for 8 minutes at 200 x g or for 10 minutes at 2500 x g to prepare platelet-rich plasma (PRP) or platelet-poor plasma (PPP), respectively. PRP and PPP

from three donors was pooled. Subsequently, 450 µL of pooled PRP was added to glass cuvettes with a stirring bar set at 1200 rpm in a Model 700 Chrono-log aggregometer (Chrono-log corporation, Havertown, USA) and maintained at 37°C. After 2 minutes, when a stable baseline was obtained, 50 µL of nanoparticle solutions in PBS were added in duplicate and light transmission was measured for 7 minutes. 450 µL of pooled PPP mixed with 50 µL PBS served as a background reference. AGGRO/LINK software (Chrono-log corporation) was used to calculate the area-under-the-curve (AUC) ranging from 2 until 9 minutes for each sample, which was expressed as a percentage of the AUC of positive control samples (1 µg/mL Collagen Reagens HORM Suspension, Takeda, Austria).

Complement activation assay. Qualitative analysis of complement activation was performed according to procedure ITA-5.1 of the NCL, with minor modifications. In brief, pooled PPP was prepared from blood (anticoagulated with 3.2% w/v trisodium citrate) from two healthy donors as described above. Pooled PPP was mixed with an equal volume of 0.2 µm filtered veronal buffer (10 mM barbital, 145 mM sodium chloride, 0.5 mM magnesium chloride, 0.15 mM calcium chloride, pH 7.2) and aliquoted in 20 µL aliquots for each sample to be tested in duplicate. Ten microliters of nanoparticle solution was added to the mixture and briefly vortexed. PBS was used as negative control, and 0.37 mg/mL of Cobra Venom Factor (CVF, Quidel Corporation, Kornwestheim, Germany) was used as a positive control. Samples were incubated for 30 minutes at 37°C. Proteins were electrotransferred to Immobilon-FL polyvinylidene difluoride (PVDF) membranes. Membranes were blocked with 50% v/v Odyssey blocking buffer (LI-COR Biosciences, Leusden, The Netherlands) in Tris-buffered saline (TBS), followed by incubation with goat anti-C3 polyclonal antibody (Protos Immunoresearch, Burlingame, USA), 1:2000 diluted in 50% v/v Odyssey blocking buffer in TBS with 0.1% v/v Tween20 (TBS-T). Blots were washed and probed with IRDye 800CW donkey anti-goat antibody (LI-COR Biosciences), 1:7500 diluted in 50% v/v Odyssey blocking buffer in TBS-T and visualized using an Odyssey Infrared Imager system (LI-COR Biosciences) at 800 nm. Band intensities of C3 cleavage products (~40 kDa) were measured with Odyssey application software (version 3.0.16, LI-COR),

normalized for lane background and expressed as a ratio compared with negative control samples.

Hemolysis assay. Hemolytic properties of nanoparticles were assessed according to procedure ITA-1 described by the NCL. In short, blood anticoagulated with lithium heparin was collected from healthy volunteers and assessed for the presence of < 1 mg/mL free plasma hemoglobin using a calibration curve of human hemoglobin (Sigma-Aldrich, Steinheim, Germany) dissolved in Drabkin's Reagent (Sigma-Aldrich), which was prepared according to the manufacturer's instructions. Whole blood was diluted to a total hemoglobin concentration of 10 mg/mL using PBS, and mixed with 8 volumes of nanoparticles in PBS in triplicates. PBS and 1% of Triton X-100 served as negative and positive controls for hemolysis, respectively. Mixtures were incubated for 3 hours at 37°C, and mixed every 30 minutes by inverting. Cells were removed by centrifuging at 800 x g for 15 minutes, and supernatants were transferred to clear 96-well plates. Sample inhibition/enhancement controls were prepared by spiking positive control supernatant with nanoparticles. All samples and controls were mixed with equal volumes of Drabkin's reagent and measured using a SpectraMax M2e microplate reader (Molecular Devices, UK) at 540 nm. Calibration curves of human hemoglobin in Drabkin's reagent were used to calculate the concentration of free hemoglobin in the supernatants. Hemolysis was expressed as the percentage of free hemoglobin compared to total blood hemoglobin.

Flow cytometry. Spleen DC maturation was assessed using CD11c-efluor610, CD11b-APC-efluor780, MHCII-efluor450, CD40-PE, CD86-APC, CD8-PE-Cy7 (all eBioscience). Quantification of OVA-specific and E7-specific CD8 T cells was performed using APC-labelled dextramers (Immudex) according to the manufacturer's instructions. CD3-BV421, CD8-PerCP-Cy5.5, IFN-γ-APC and TNF-α-PE-Cy7 (all BD Biosciences) were used for intracellular cytokine staining using the BD Cytofix/Cytoperm kit (BD Biosciences) according to the manufacturer's instructions. The data were collected using the LSRFortessa or FACSCanto (BD) and the analysis of the data was performed using the FACSDiva (BD) and Flow Jo software.

Confocal imaging. Confocal imaging was performed on spleen sections from C57BL/6 WT mice obtained from Harlan or from Rosa x tdRFP mice. The following antibodies were used: CD3e (145-2C11) was purchased from Tonbo Biosciences. CD11c (HL3), CD11b (M1/70) and B220 (RA3-6B2) were obtained from BD Biosciences. CD169 (MOMA-1) was obtained from Serotec Bio-Rad. Briefly, 7-µm spleen frozen sections were fixed for 4 min in PFA 2%. After washing with PBS, sections were stained with the primary antibodies for 60 min at room temperature, followed by a 30-min incubation period with secondary antibodies (obtained from Invitrogen; catalog numbers A11008 and A-11090 and Jackson ImmunoResearch; catalog number 712-166-153). Sections were counterstained with DAPI. Images were acquired on a Zeiss LSM710 confocal microscope equipped with 488-nm, 561-nm and 633-nm lasers and with a tunable two-photon laser. Images were analyzed with Imaris software.

Enzyme-Linked Immunosorbent Assay. Blood was collected after immunization at the indicated time points. The serum of the collected blood was screened for the presence of IFN-α using the VeriKine Mouse IFN Alpha ELISA Kit (pbl assay science, USA).

ELISPOT. ELISPOT was performed to measure IFN-γ production by splenocytes isolated 5 days post immunization. The ELISPOT was performed as described.[41]

Cytokine measurements. Murine serum cytokine titers were determined using a custom-made mouse Procartaplex 8-plex kit (Life Technologies Europe BV). Samples were measured on a Bio-Plex 200 system (BioRAD).

Tumor experiments. Mice were inoculated subcutaneously with 2 x 10^5 TC-1 tumor or 2 x 10^5 B16-OVA tumor cells in 50 µl PBS in the right flank. Ten days post injection, the mice were randomly assigned to the distinct immunization groups.

Statistical analysis. Evaluation of two data sets was done using the unpaired student's t-test. Evaluation of more than 2 groups was done using a one or two-way ANOVA. The graphs display the results as the mean ± SEM. Survival graphs are visualized as Kaplan-Meier plots and analyzed using the log-rank test. The number of asterisks

indicates the level of statistical significance as follows: *, $p < 0.05$; **, $p < 0.01$; ***, $p < 0.001$.

ACKNOWLEDGEMENTS

We thank P. Roman, E. Vaeremans, E. Heirman, E. De Smet, J. Corthals, J. Puttemans, C. Mahmoud and F. Geldholf for their technical assistance. We thank C. Goyvaerts for the breeding of transgenic mice and M. Keyaerts to provide the bioluminescence device. We thank S. Akhter, A. Sauldubois and C. Andreazza from the "Centre de Microscopie Electronique" of University of Orléans, France for assistance in TEM data acquisition. This work was supported by grants from the Interuniversity Attraction Poles Program-Belgian State- Belgian Science Policy, the National Cancer Plan of the Federal Ministry of Health, the Stichting tegen Kanker, the Vlaamse Liga tegen Kanker, an Integrated Project and an EU FP7-funded Network of Excellence, an IWT-TBM program, the FWO-Vlaanderen, Fonds Germaine Eisendrath-Dubois and the Scientific Fund Willy Gepts of the University Hospital Brussels. KVdJ, LB, PTJ and KB are supported by the IWT. The production of mRNA was supported by eTheRNA immunotherapies, a spin-off company of the Vrije Universiteit Brussel, founded by K. Thielemans.

Author contributions: Study design: KVdJ, SDK, PM, KBreckpot, KT. Data acquisition: KVdJ, SDK, LB, PTJ, SB, KBroos, KD, PB. Analysis and interpretation: KVdJ, SDK, CH, CP, PM, KBreckpot, KT. Manuscript drafting: KVdJ, SDK, KBreckpot. Manuscript correction: KVdJ, SDK, LB, CH, PTJ, SB, KBroos, KD, VM, TB, SL, PAJ, BL, PB, CP, PM, KBreckpot, KT.

Competing interests: A patent was filed based on the current study: Application No. 17181865.1-1403. K. Van der Jeught, S. De Koker, C. Pichon, P. Midoux, K. Breckpot and K. Thielemans are listed as inventors on the patent. K. Thielemans is also an inventor on the patented TriMix vaccine. The patents have been licensed to a biotech company.

ASSOCIATED CONTENT

Supporting Information.

Supporting Information Available. Details on mRNA and polymer incorporation in the LPR, biodistribution of Cy5 mRNA, bioluminescence distribution signal of LR *versus* LPR, flow cytometry gating strategy, vaccine dose dependency OVA-dextramer and IFN-γ ELISPOT, nanoparticle structure and their respective capacity to induce immune responses, comparison of survival of LPR with *ex vivo* DC vaccination, cytokine responses of LPR with unmodified and N1mψ modified mRNA, biodistribution and systemic release of IFN-α kinetics, transfection efficiency and viability of human monocyte derived DCs. This material is available free of charge *via* the Internet at http://pubs.acs.org.

AUTHOR INFORMATION

Corresponding Authors

*E-mail: kris.thielemans@vub.ac.be

*E-mail: kbreckpo@vub.ac.be

*E-mail: chantal.pichon@cnrs.fr

ORCID ID

Kevin Van der Jeught: 0000-0002-4626-2343

REFERENCES:

(1) Broos, K.; Van der Jeught, K.; Puttemans, J.; Goyvaerts, C.; Heirman, C.; Dewitte, H.; Verbeke, R.; Lentacker, I.; Thielemans, K.; Breckpot, K., Particle-Mediated Intravenous Delivery of Antigen mRNA Results in Strong Antigen-Specific T-Cell Responses Despite the Induction of Type I Interferon. *Mol. Ther. Nucleic Acids* **2016,** *5*, e326.

(2) Kranz, L. M.; Diken, M.; Haas, H.; Kreiter, S.; Loquai, C.; Reuter, K. C.; Meng, M.; Fritz, D.; Vascotto, F.; Hefesha, H.; Grunwitz, C.; Vormehr, M.; Husemann, Y.; Selmi, A.; Kuhn, A. N.; Buck, J.; Derhovanessian, E.; Rae, R.; Attig, S.; Diekmann, J.; Jabulowsky, R. A; *et al*., Systemic RNA Delivery to Dendritic Cells Exploits Antiviral Defence for Cancer Immunotherapy. *Nature* **2016,** *534*, 396-401.

(3) Pektor, S.; Bausbacher, N.; Otto, G.; Lawaczeck, L.; Grabbe, S.; Schreckenberger, M.; Miederer, M., Toll Like Receptor Mediated Immune Stimulation can be Visualized *in vivo* by [18F]FDG-PET. *Nucl. Med. Biol*. **2016,** *43*, 651-660.

(4) Zhang, J. S.; Liu, F.; Huang, L., Implications of Pharmacokinetic Behavior of Lipoplex for its Inflammatory Toxicity. *Adv. Drug Delivery Rev*. **2005,** *57*, 689-98.

(5) Xue, H. Y.; Liu, S.; Wong, H. L., Nanotoxicity: a Key Obstacle to Clinical Translation of siRNA-Based Nanomedicine. *Nanomedicine* **2014,** *9*, 295-312.

(6) Zatsepin, T. S.; Kotelevtsev, Y. V.; Koteliansky, V., Lipid Nanoparticles for Targeted siRNA Delivery - Going From Bench to Bedside. *Int. J. Nanomed*. **2016,** *11*, 3077-86.

(7) Kormann, M. S.; Hasenpusch, G.; Aneja, M. K.; Nica, G.; Flemmer, A. W.; Herber-Jonat, S.; Huppmann, M.; Mays, L. E.; Illenyi, M.; Schams, A.; Griese, M.; Bittmann, I.; Handgretinger, R.; Hartl, D.; Rosenecker, J.; Rudolph, C., Expression of Therapeutic Proteins after Delivery of Chemically Modified mRNA in Mice. *Nat. Biotechnol*. **2011,** *29*, 154-7.

(8) Kariko, K.; Muramatsu, H.; Welsh, F. A.; Ludwig, J.; Kato, H.; Akira, S.; Weissman, D., Incorporation of Pseudouridine into mRNA Yields Superior Nonimmunogenic Vector with Increased Translational Capacity and Biological Stability. *Mol. Ther*. **2008,** *16*, 1833-40.

(9) Andries, O.; Mc Cafferty, S.; De Smedt, S. C.; Weiss, R.; Sanders, N. N.; Kitada, T., N(1)-Methylpseudouridine-Incorporated mRNA Outperforms Pseudouridine-Incorporated mRNA by

Providing Enhanced Protein Expression and Reduced Immunogenicity in Mammalian Cell Lines and Mice. *J. Controlled release* **2015,** *217*, 337-44.

(10) Crow, M. K., Type I Interferon in the Pathogenesis of Lupus. *J. Immunol.* **2014,** *192*, 5459-68.

(11) Rizza, P.; Moretti, F.; Belardelli, F., Recent Advances on the Immunomodulatory Effects of IFN-Alpha: Implications for Cancer Immunotherapy and Autoimmunity. *Autoimmunity* **2010,** *43*, 204-9.

(12) Pott, J.; Stockinger, S., Type I and III Interferon in the Gut: Tight Balance between Host Protection and Immunopathology. *Front. Immunol.* **2017,** *8*, 258.

(13) Rezaee, M.; Oskuee, R. K.; Nassirli, H.; Malaekeh-Nikouei, B., Progress in the Development of Lipopolyplexes as Efficient Non-Viral Gene Delivery Systems. *J. Controlled Release* **2016,** *236*, 1-14.

(14) Goncalves, C.; Berchel, M.; Gosselin, M. P.; Malard, V.; Cheradame, H.; Jaffres, P. A.; Guegan, P.; Pichon, C.; Midoux, P., Lipopolyplexes Comprising Imidazole/Imidazolium Lipophosphoramidate, Histidinylated Polyethyleneimine and siRNA as Efficient Formulation for siRNA Transfection. *Int. J. Pharm.* **2014,** *460*, 264-72.

(15) Perche, F.; Benvegnu, T.; Berchel, M.; Lebegue, L.; Pichon, C.; Jaffres, P. A.; Midoux, P., Enhancement of Dendritic Cells Transfection *In Vivo* and of Vaccination Against B16F10 Melanoma with Mannosylated Histidylated Lipopolyplexes Loaded with Tumor Antigen Messenger RNA. *Nanomedicine* **2011,** *7*, 445-53.

(16) Barbeau, J.; Lemiegre, L.; Quelen, A.; Malard, V.; Gao, H.; Goncalves, C.; Berchel, M.; Jaffres, P. A.; Pichon, C.; Midoux, P.; Benvegnu, T., Synthesis of a Trimannosylated-Equipped Archaeal Diether Lipid for the Development of Novel Glycoliposomes. *Carbohydr. Res.* **2016,** *435*, 142-148.

(17) Wang, Y.; Su, H. H.; Yang, Y.; Hu, Y.; Zhang, L.; Blancafort, P.; Huang, L., Systemic Delivery of Modified mRNA Encoding Herpes Simplex Virus 1 Thymidine Kinase for Targeted Cancer Gene Therapy. *Mol. Ther.* **2013,** *21*, 358-67.

(18) Luche, H.; Weber, O.; Nageswara Rao, T.; Blum, C.; Fehling, H. J., Faithful Activation of an Extra-Bright Red Fluorescent Protein in "Knock-In" Cre-Reporter Mice Ideally Suited for Lineage Tracing Studies. *Eur. J. Immunol.* **2007,** *37*, 43-53.

(19) Mildner, A.; Jung, S., Development and Function of Dendritic Cell Subsets. *Immunity* **2014,** *40*, 642-56.

(20) Li, L.; Kim, S.; Herndon, J. M.; Goedegebuure, P.; Belt, B. A.; Satpathy, A. T.; Fleming, T. P.; Hansen, T. H.; Murphy, K. M.; Gillanders, W. E., Cross-Dressed CD8Alpha+/CD103+ Dendritic Cells Prime CD8+ T Cells Following Vaccination. *Proc. Natl. Acad. Sci. U. S. A.* **2012,** *109*, 12716-21.

(21) Durward, M.; Harms, J.; Splitter, G., Antigen Specific Killing Assay Using CFSE Labeled Target Cells. *J. Visualized Exp.* **2010,** 45.

(22) Bonehill, A.; Tuyaerts, S.; Van Nuffel, A. M.; Heirman, C.; Bos, T. J.; Fostier, K.; Neyns, B.; Thielemans, K., Enhancing the T-Cell Stimulatory Capacity of Human Dendritic Cells by Co-Electroporation with CD40L, CD70 and Constitutively Active TLR4 Encoding mRNA. *Mol. Ther.* **2008,** *16*, 1170-80.

(23) Van Lint, S.; Wilgenhof, S.; Heirman, C.; Corthals, J.; Breckpot, K.; Bonehill, A.; Neyns, B.; Thielemans, K., Optimized Dendritic Cell-Based Immunotherapy for Melanoma: the TriMix-Formula. *Cancer Immunol. Immunother.* **2014,** *63*, 959-67.

(24) Han, Q.; Bagheri, N.; Bradshaw, E. M.; Hafler, D. A.; Lauffenburger, D. A.; Love, J. C., Polyfunctional Responses by Human T Cells Result from Sequential Release of Cytokines. *Proc. Natl. Acad. Sci. U. S. A.* **2012,** *109*, 1607-12.

(25) Mockey, M.; Bourseau, E.; Chandrashekhar, V.; Chaudhuri, A.; Lafosse, S.; Le Cam, E.; Quesniaux, V. F.; Ryffel, B.; Pichon, C.; Midoux, P., mRNA-Based Cancer Vaccine: Prevention of B16 Melanoma Progression and Metastasis by Systemic Injection of MART1 mRNA Histidylated Lipopolyplexes. *Cancer Gene Ther.* **2007,** *14*, 802-14.

(26) Wilgenhof, S.; Corthals, J.; Heirman, C.; van Baren, N.; Lucas, S.; Kvistborg, P.; Thielemans, K.; Neyns, B., Phase II Study of Autologous Monocyte-Derived mRNA Electroporated Dendritic Cells (TriMixDC-MEL) Plus Ipilimumab in Patients With Pretreated Advanced Melanoma. *J. Clin. Oncol.* **2016,** *34*, 1330-8.

(27) Lienenklaus, S.; Cornitescu, M.; Zietara, N.; Lyszkiewicz, M.; Gekara, N.; Jablonska, J.; Edenhofer, F.; Rajewsky, K.; Bruder, D.; Hafner, M.; Staeheli, P.; Weiss, S., Novel Reporter Mouse Reveals Constitutive and Inflammatory Expression of IFN-Beta *In Vivo*. *J. Immunol.* **2009,** *183*, 3229-36.

(28) Donovan, J.; Dufner, M.; Korennykh, A., Structural Basis for Cytosolic Double-Stranded RNA Surveillance by Human Oligoadenylate Synthetase 1. *Proc. Natl. Acad. Sci. U. S. A.* **2013,** *110*, 1652-7.

(29) Anderson, B. R.; Muramatsu, H.; Jha, B. K.; Silverman, R. H.; Weissman, D.; Kariko, K., Nucleoside Modifications in RNA Limit Activation of 2'-5'-Oligoadenylate Synthetase and Increase Resistance to Cleavage by RNase L. *Nucleic Acids Res.* **2011,** *39*, 9329-38.

(30) Anderson, B. R.; Muramatsu, H.; Nallagatla, S. R.; Bevilacqua, P. C.; Sansing, L. H.; Weissman, D.; Kariko, K., Incorporation of Pseudouridine into mRNA Enhances Translation by Diminishing PKR Activation. *Nucleic Acids Res.* **2010,** *38*, 5884-92.

(31) Kariko, K.; Buckstein, M.; Ni, H.; Weissman, D., Suppression of RNA Recognition by Toll-Like Receptors: the Impact of Nucleoside Modification and the Evolutionary Origin of RNA. *Immunity* **2005,** *23*, 165-75.

(32) Kariko, K.; Muramatsu, H.; Keller, J. M.; Weissman, D., Increased Erythropoiesis in Mice Injected with Submicrogram Quantities of Pseudouridine-Containing mRNA Encoding Erythropoietin. *Mol. Ther.* **2012,** *20*, 948-53.

(33) Kariko, K.; Muramatsu, H.; Ludwig, J.; Weissman, D., Generating the Optimal mRNA for Therapy: HPLC Purification Eliminates Immune Activation and Improves Translation of Nucleoside-Modified, Protein-Encoding mRNA. *Nucleic Acids Res.* **2011,** *39*, e142.

(34) Zangi, L.; Lui, K. O.; von Gise, A.; Ma, Q.; Ebina, W.; Ptaszek, L. M.; Spater, D.; Xu, H.; Tabebordbar, M.; Gorbatov, R.; Sena, B.; Nahrendorf, M.; Briscoe, D. M.; Li, R. A.; Wagers, A. J.; Rossi, D. J.; Pu, W. T.; Chien, K. R., Modified mRNA Directs the Fate of Heart Progenitor Cells and Induces Vascular Regeneration After Myocardial Infarction. *Nat. Biotechnol.* **2013,** *31*, 898-907.

(35) Kauffman, K. J.; Mir, F. F.; Jhunjhunwala, S.; Kaczmarek, J. C.; Hurtado, J. E.; Yang, J. H.; Webber, M. J.; Kowalski, P. S.; Heartlein, M. W.; DeRosa, F.; Anderson, D. G., Efficacy and

Immunogenicity of Unmodified and Pseudouridine-Modified mRNA Delivered Systemically with Lipid Nanoparticles *In Vivo*. *Biomaterials* **2016,** *109*, 78-87.

(36) Stadler, C. R.; Bahr-Mahmud, H.; Celik, L.; Hebich, B.; Roth, A. S.; Roth, R. P.; Kariko, K.; Tureci, O.; Sahin, U., Elimination of Large Tumors in Mice by mRNA-Encoded Bispecific Antibodies. *Nat. Med.* **2017,** *23*, 815-817.

(37) Svitkin, Y. V.; Cheng, Y. M.; Chakraborty, T.; Presnyak, V.; John, M.; Sonenberg, N., N1-Methyl-Pseudouridine in mRNA Enhances Translation through eIF2alpha-Dependent and Independent Mechanisms by Increasing Ribosome Density. *Nucleic Acids Res.* **2017,** *45*, 6023-6036.

(38) Sultana, N.; Magadum, A.; Hadas, Y.; Kondrat, J.; Singh, N.; Youssef, E.; Calderon, D.; Chepurko, E.; Dubois, N.; Hajjar, R. J.; Zangi, L., Optimizing Cardiac Delivery of Modified mRNA. *Mol. Ther.* **2017,** *25*, 1306-1315.

(39) Ramaswamy, S.; Tonnu, N.; Tachikawa, K.; Limphong, P.; Vega, J. B.; Karmali, P. P.; Chivukula, P.; Verma, I. M., Systemic Delivery of Factor IX Messenger RNA for Protein Replacement Therapy *Proc. Natl. Acad. Sci. U. S. A.* **2017,** *114*, E1941-e1950.

(40) Van Lint, S.; Goyvaerts, C.; Maenhout, S.; Goethals, L.; Disy, A.; Benteyn, D.; Pen, J.; Bonehill, A.; Heirman, C.; Breckpot, K.; Thielemans, K., Preclinical Evaluation of TriMix and Antigen mRNA-Based Antitumor Therapy. *Cancer Res.* **2012,** *72*, 1661-71.

(41) Bialkowski, L.; van Weijnen, A.; Van der Jeught, K.; Renmans, D.; Daszkiewicz, L.; Heirman, C.; Stange, G.; Breckpot, K.; Aerts, J. L.; Thielemans, K., Intralymphatic mRNA Vaccine Induces CD8 T-Cell Responses that Inhibit the Growth of Mucosally Located Tumours. *Sci. Rep.* **2016,** *6*, 22509.

(42) Mevel, M.; Breuzard, G.; Yaouanc, J. J.; Clement, J. C.; Lehn, P.; Pichon, C.; Jaffres, P. A.; Midoux, P., Synthesis and Transfection Activity of New Cationic Phosphoramidate Lipids: High Efficiency of an Imidazolium Derivative. *Chembiochem* **2008,** *9*, 1462-71.

(43) Monsigny, M.; Petit, C.; Roche, A. C., Colorimetric Determination of Neutral Sugars by a Resorcinol Sulfuric Acid Micromethod. *Anal. Biochem.* **1988,** *175*, 525-30.

(44) Midoux, P.; Monsigny, M., Efficient Gene Transfer by Histidylated Polylysine/pDNA Complexes. *Bioconjugate Chem.* **1999,** *10*, 406-11.

(45) Bialkowski, L.; Van der Jeught, K.; Renmans, D.; van Weijnen, A.; Heirman, C.; Keyaerts, M.; Breckpot, K.; Thielemans, K., Adjuvant-Enhanced mRNA Vaccines. *Methods Mol. Biol.* **2017,** *1499*, 179-191.

FIGURE CAPTIONS

Figure 1. LPR generation and characterization. (A) LPR nanoparticles are formed in a 2-step process. In a first step, the PEG-HpK polymer is added to the mRNA, thereby forming an mRNA polyplex. In a second step, the TriMan-liposome is added to the polyplex, thereby forming a lipopolyplex (LPR). The table depicts the hydrodynamic diameter and Z-potential of LPR made from OVA or E7 mRNA (n=3) as measured by Dynamic Light Scattering (DLS). **(B)** Chemical structures of the LPR components. **(C)** Electric mobility shift assay of free mRNA or LPR with or without serum exposure. Ladder (1), Endofree Water (2), Free mRNA (3), LPR (4), Serum exposed LPR (5) and Free mRNA (6). **(D)** Agilent capillary gel electrophoresis on TRizol incubated non-encapsulated mRNA and LPR encapsulated mRNA. **(E-G)** Morphological observations by transmission electron miroscopy of **(E)** TriMan liposomes, **(F)** mRNA:PEG-HpK at 1/3 weight ratio and **(G)** LPR in the ratio 1/3/2 after negative staining with 2% uranyl acetate. Scale bar: 100 nm.

Figure 2. Systemic LPR administration targets and activates splenic DCs. (A-B) Bioluminescence imaging (BLI) was performed 24 hours after the intravenous administration of 20 µg Fluc mRNA as LPR (n = 9). The whole body BLI is depicted in **(A)** and the organs isolated after 24 hours are shown in **(B).** BLI of isolated organs 1) spleen 2) lung 3) liver 4) inguinal lymph nodes 5) intestines 6) kidney 7) heart 8) stomach. **(C)** Intensity of bioluminescence in spleens of CD11c-DTR mice after injection of Fluc mRNA LPR (20 µg mRNA). – DT = without Diphtheria Toxin; + DT = with Diphtheria Toxin. Data are a representative of two independent experiments (n = 4). * $P < 0.05$ (Unpaired t-test). **(D)** Immunohistochemistry images of spleen sections after injection of *ROSA26-loxP-Stop-loxP RFP* transgenic mice with Cre mRNA LPR (n = 4) Spleens were stained for MOMA-1 and for CD11c to visualize metallophilic marginal zone macrophages and DCs. Triangles in R1 indicate RFP expression in MOMA-1+ cells whereas arrows in R2 indicate RFP expression in CD11c + cells **(E)** Flow cytometric analysis of the expression of MHCII, CD86 and CD40 on splenic CD8a DCs and CD11b DCs after IV injection of PBS (untreated) or Fluc mRNA LPR. Data are

shown as means +/- SD (n = 4). **** P < 0.0001; ns = non-significant (Two-Way ANOVA Analysis followed by Bonferroni's multiple comparisons test).

Figure 3. Systemic LPR administration instigates potent T-cell immunity. (A) Cytolytic T-cell response as measured by the % target cell lysis after single immunization with LPR. Mice were immunized with OVA mRNA (10 µg) or E7 mRNA (10 µg) supplemented with either irrelevant control mRNA (15 µg) or with TriMix mRNA (5 µg/component). Data are shown as means +/- SD and are a representative of two independent experiments (n = 4). **P < 0.01; * p < 0.05 (Two-way ANOVA followed by Bonferroni's multiple comparisons test). **(B)** Schematic overview of the immunization and sampling schedule applied. Mice were immunized at days 0, 7, 14 and 60 with OVA/TriMix (10 µg/15 µg) mRNA LPR. Blood samples were collected for quantification of the percentages of OVA-specific CD8 T cells at days 0, 5, 12, 19, 35, 55 and 65. Spleens were collected at day 65 for quantification of IFN-γ and TNF-α production by OVA-specific CD8 T cells. Flow cytometry analysis of the percentages of circulating OVA-specific CD8 T cells. **(C)** Flow cytometry analysis of cytokine production by OVA-specific T cells with (red) and without *ex vivo* peptide (blue) re-stimulation. Percentages of IFN-γ+, TNF-α+ and IFN-γ+ TNF-α+ OVA-specific CD8 T cells. Results are shown as means +/- SD (n =6). **** P < 0.0001; ns = non-significant (Two-way ANOVA followed by Bonferroni's multiple comparisons test).

Figure 4.Systemic LPR administration elicits profound antitumor immunity. (A) TC-1 inoculation and treatment schedule. Mice were immunized with E7/TriMix (10 µg/15 µg) mRNA LR or LPR. **(B)** Spaghetti plots showing tumor growth rates of individual mice.

Figure 5. LPR induced type I IFN are dispensable for cytolytic T-cell differentiation. (A) Serum IFN-α titers as measured by ELISA at the indicated time intervals after systemic administration of LPR (25 µg Fluc mRNA). Data are shown as means +/- SD (n = 4). *** P < 0.001; ** p < 0.01; ns = non-significant (One-way ANOVA analysis followed by Bonferroni's multiple comparisons test). **(B)** *In vivo* BLI images showing the anatomical distribution of IFN-β activation as reflected by luciferase expression in the IFN-β reporter mice. Mice were injected with 25 µg OVA mRNA (n=3).

(C) NanoString transcriptome profiling of spleens three hours after systemic LPR administration. **(D-F)** Cytolytic T-cell responses as measured by the % target cell lysis in wild type mice and Ifnar$^{-/-}$ mice after single immunization with LPR containing respectively OVA/TriMix mRNA **(D)**, OVA/ctrl mRNA **(E)** or with LR containing OVA/TriMix mRNA **(F)**. Data are shown as means +/- SD (n= 4-8). Data shown are a representative of three independent experiments. *** P < 0.001; ns = non-significant (unpaired t-test).

Figure 6. N1mψ modified mRNA reduces inflammatory responses to systemic LPR immunization. (A-B) Quantification of inflammatory cytokine responses in blood of LPR injected mice relative to untreated mice at two hours and six hours' post injection. **(A)** Heat map representation after injection of unmodified Fluc mRNA LPR (25 µg mRNA) and N1mψ nucleoside modified Fluc mRNA LPR (25 µg mRNA). **(B)** Graphs showing the differential induction of IFN-α, CXCL-10, IL-12 and IL-6 to unmodified mRNA LPR and N1mψ mRNA LPR. Data are shown as $\log_2$ fold change in titers when compared to untreated mice. Data are shown as means +/- SD (n = 4). **** P < 0.0001; *** p < 0.001; ** p < 0.01; ns = non-significant (Two-way ANOVA followed by Bonferroni's multiple comparisons test. **(C)** *In vivo* BLI images showing similar anatomical distribution and reduced intensity of IFN-β activation in N1mψ mRNA LPR as reflected by luciferase expression in the IFN-β reporter mice. Mice were injected with 25 µg OVA mRNA (n=3). **(D)** IFN-α and IFN-β titers in supernatants of human PBMCs incubated with the indicated doses of unmodified Fluc mRNA LPR and N1mψ Fluc mRNA LPR.

Figure 7. N1mψ nucleoside modified mRNA does not hamper antitumor T-cell immunity to LPR. (A-C) Flow cytometry analysis of antigen-specific T cells upon immunization with respectively unmodified mRNA or N1mψ mRNA LPR. **(A)** Schematic overview of immunization and sampling schedule **(B)** Representative flow cytometry plots depicting the percentages of OVA-specific T cells after the third immunization with unmodified mRNA or N1mψ mRNA LPR. **(C)** Percentages of OVA-specific CD8 T cells (*left panel*) and E7-specific CD8 T cells *(right panel*) after the second and third immunization with unmodified mRNA or N1mψ mRNA LPR. (n=8). **(D)** The graph

depicts the percentage of IFN-γ positive OVA specific CD8 T cells (n=6). **(E-F)** Percentages target cell lysis upon single immunization with LPR that contain either unmodified mRNA or N1mψ modified mRNA. **(E)** Percentages of target cell lysis after immunization with LPR and LR. LPR and LR contained the Tri-mannosylated liposomes used throughout the study. Data are shown as means +/- SD (n = 8). **(F)** Percentages of target cell lysis after immunization with RNAiMAX LPR and RNAiMAX LR. **(G)** The percentage of E7 specific CD8 T cells are shown after three immunizations with the indicated nanoparticle (LR or LPR) and (unmodified or N1mψ) mRNA (n=3) **(H-J)** Tumor growth curves of TC-1 and B16-OVA inoculated mice treated as depicted by IV immunization. TC-1 mice received three immunizations with E7/TriMix mRNA LPR. B16-OVA mice received three immunizations with OVA/TriMix mRNA LPR. Data are shown as means +/- SD (H: n=7, I-J: n=8). Ns = non- significant; *** $p < 0,001$; ** $p < 0.01$; * $p < 0.05$.

Figure 8. Characterization of LPR hemocompatibility on human blood. (A) Analysis of complement activation by Western Blot. Isolated platelet poor plasma of healthy donors was incubated with LPR at the indicated mRNA concentrations. Cobra Venom factor (CVF) was used as a positive control. SDS PAGE gels were stained with a polyclonal antibody for C3a to quantify C3a cleavage. Cleavage product band intensity was quantified and compared with PBS control. **(B)** Graph showing the relative increase in cleaved C3a/uncleaved C3a ratio compared to PBS. **(C)** Quantification of the percentage hemolysis upon incubation of Li-heparin anticoagulated blood obtained from two different healthy donors with LPR at the indicated mRNA concentrations. **(D)** Quantification of platelet aggregation. Platelet aggregation was assessed on pooled platelet rich plasma from three healthy donors using a Chrono-LOG aggregometer. Collagen was used as positive control. **(E)** IFN-α and **(F)** IFN-β titers in supernatans of human PBMCs incubated with the indicated doses of unmodified Fluc mRNA LPR and N1mψ Fluc mRNA LPR.

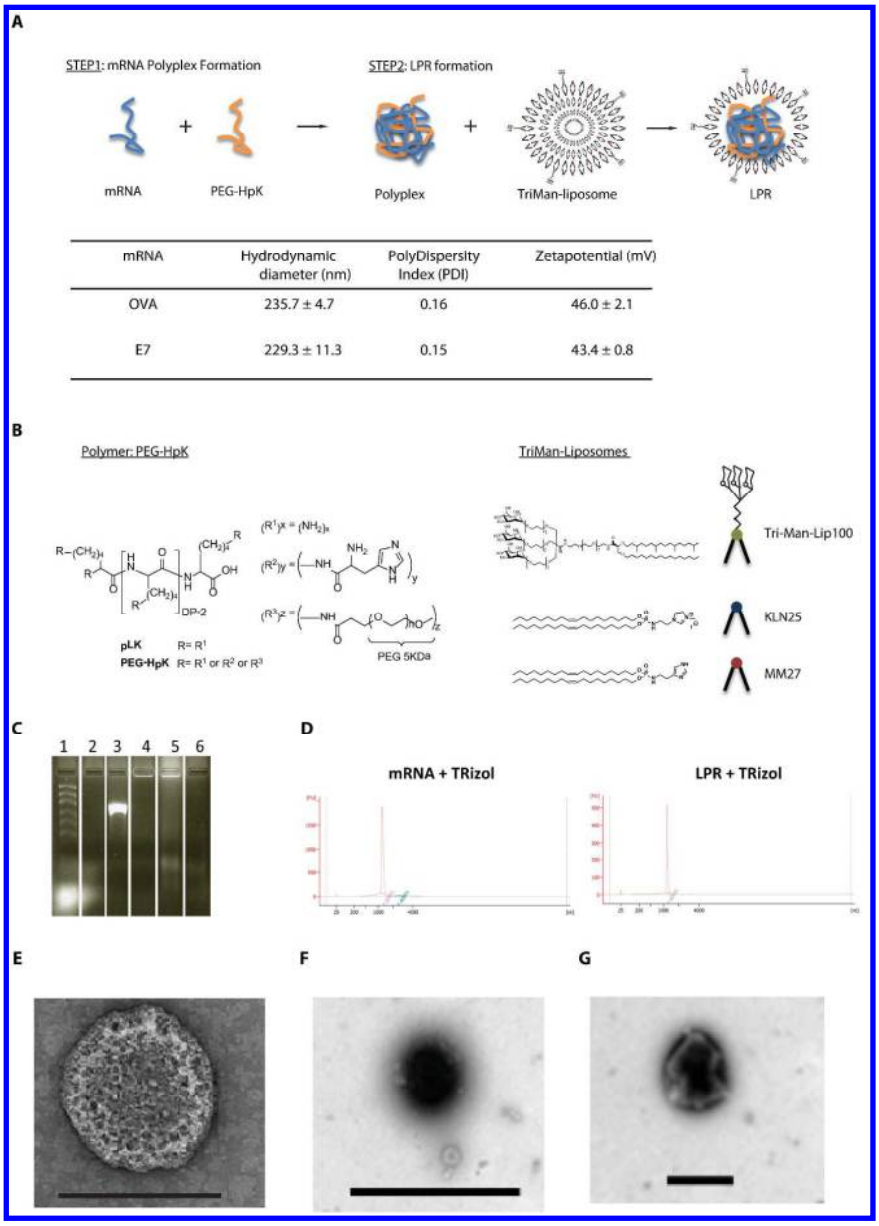

mRNA	Hydrodynamic diameter (nm)	PolyDispersity Index (PDI)	Zetapotential (mV)
OVA	235.7 ± 4.7	0.16	46.0 ± 2.1
E7	229.3 ± 11.3	0.15	43.4 ± 0.8

Figure 1. LPR generation and characterization.

272x380mm (300 x 300 DPI)

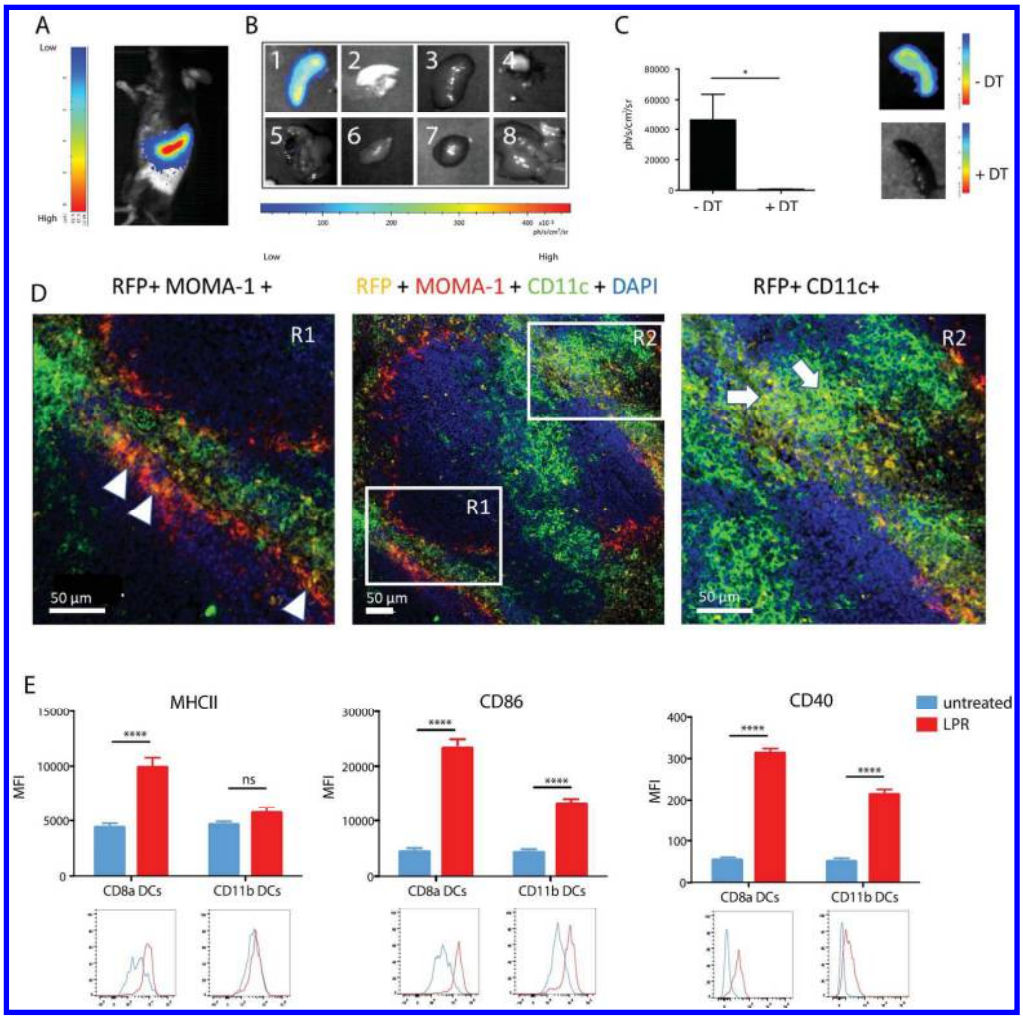

Figure 2. Systemic LPR administration targets and activates splenic DCs.

182x181mm (300 x 300 DPI)

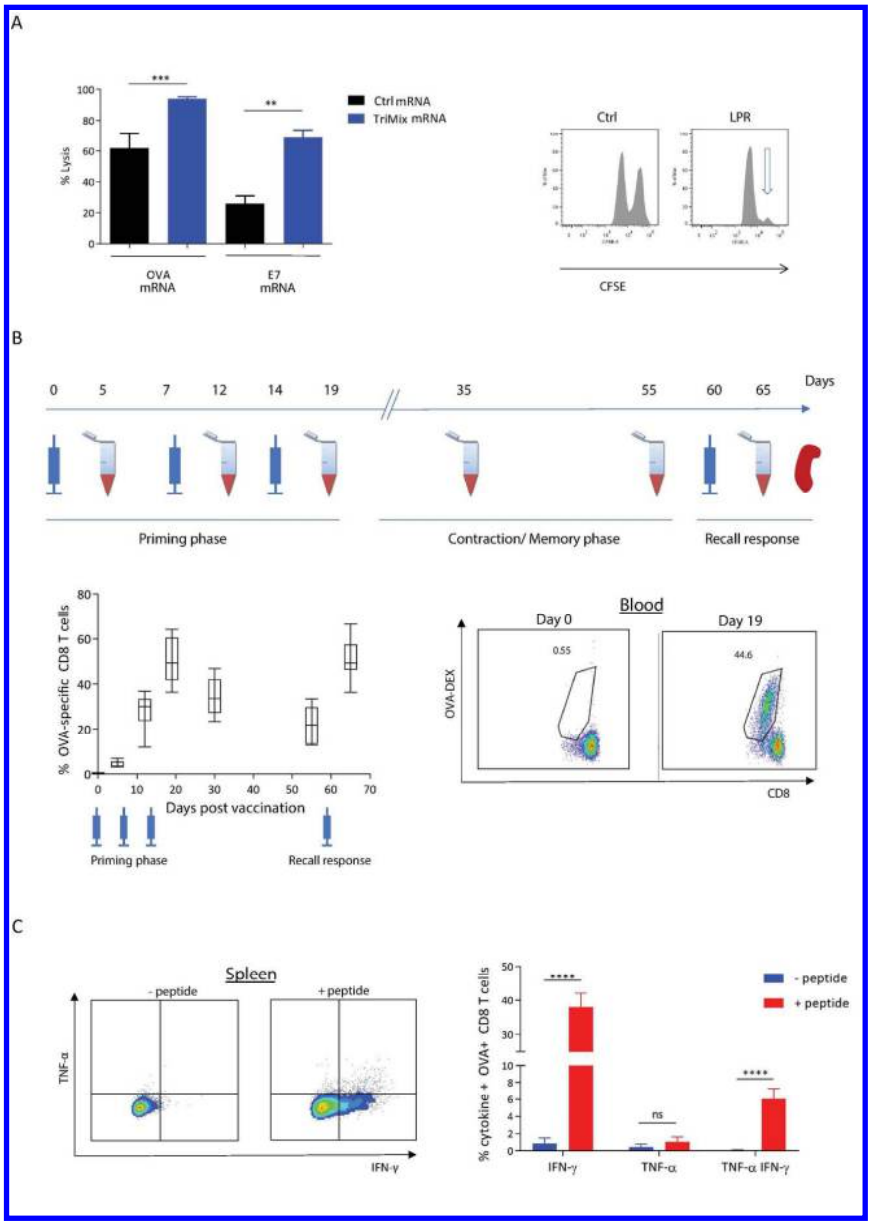

Figure 3. Systemic LPR administration instigates potent T-cell immunity.

161x228mm (300 x 300 DPI)

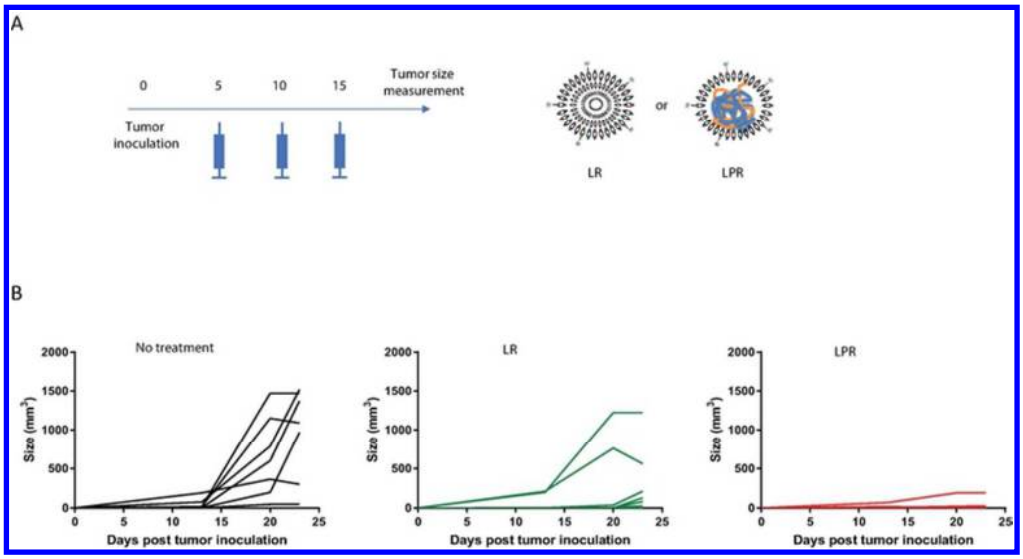

Figure 4.Systemic LPR administration elicits profound antitumor immunity

66x35mm (300 x 300 DPI)

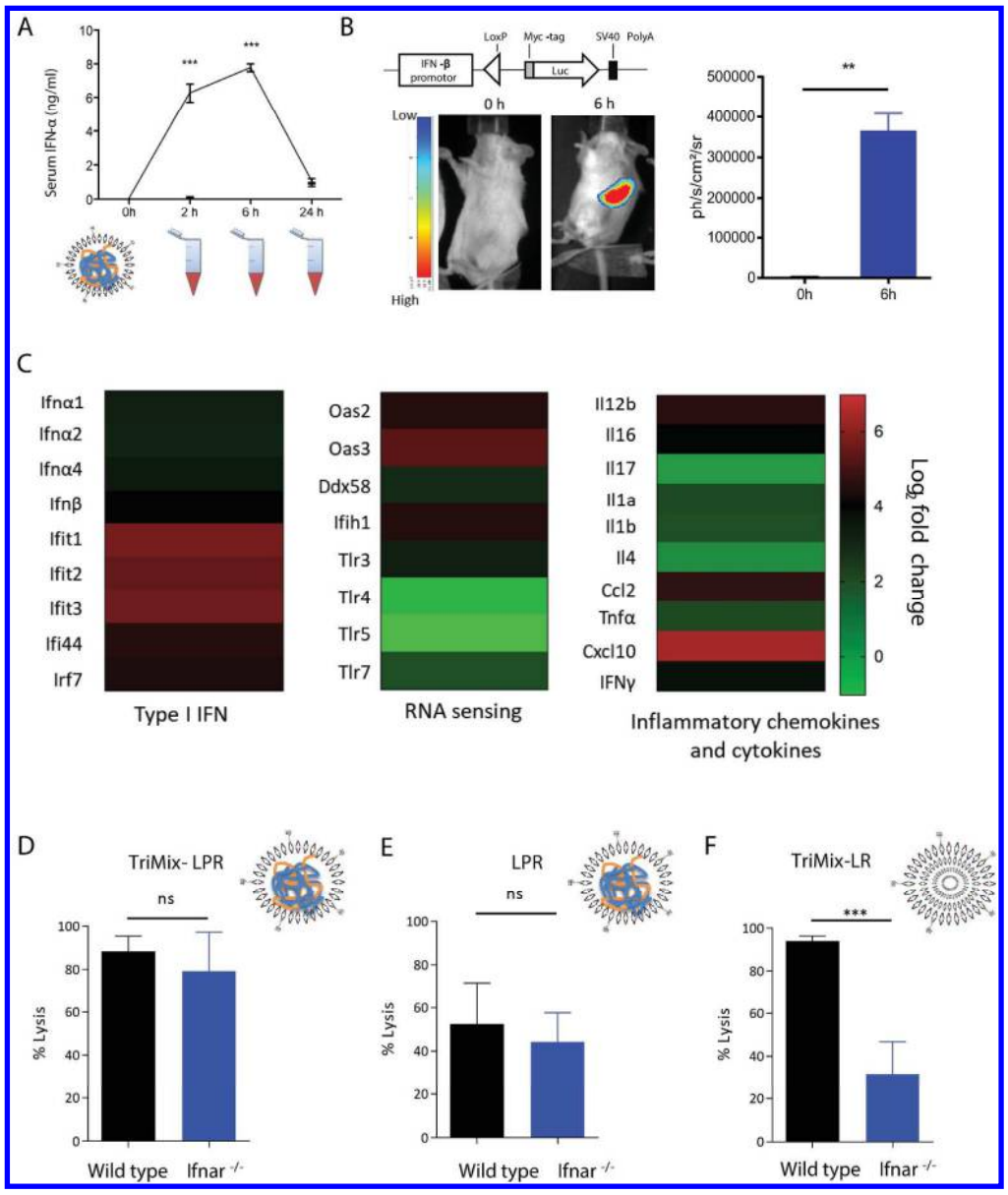

Figure 5. LPR induced type I IFN are dispensable for cytolytic T-cell differentiation

243x289mm (300 x 300 DPI)

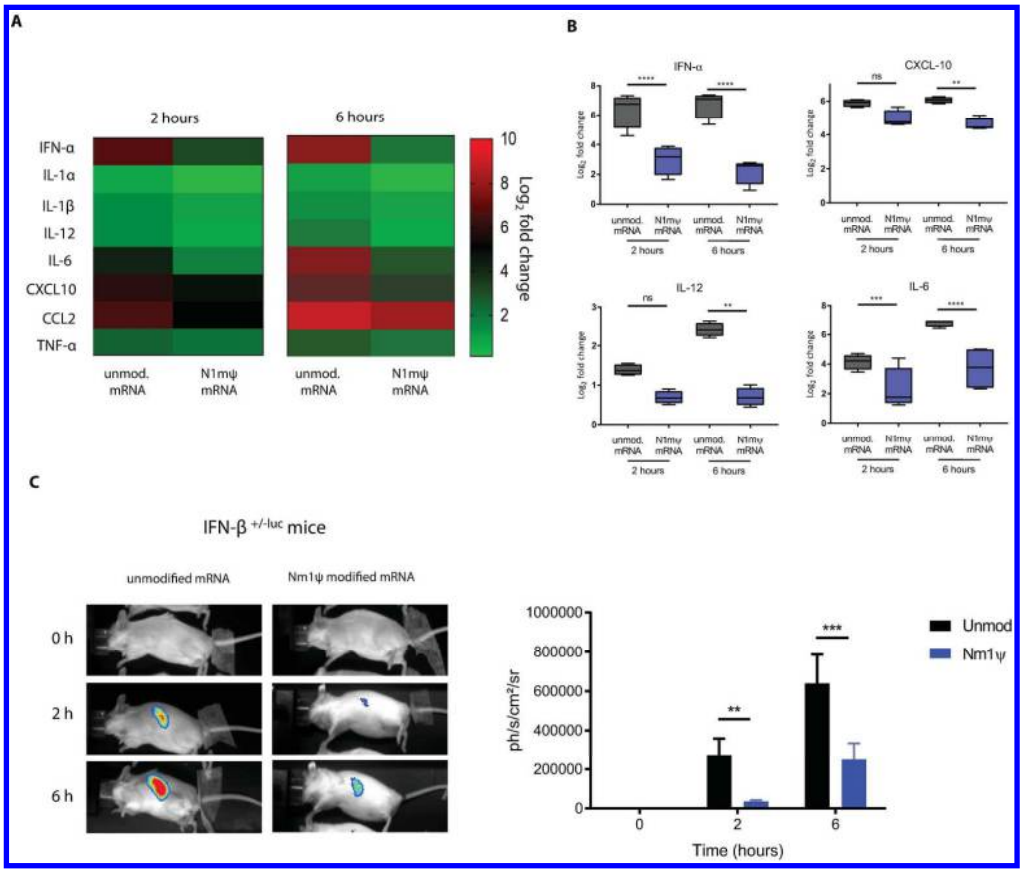

Figure 6. N1mψ modified mRNA reduces inflammatory responses to systemic LPR immunization

172x146mm (300 x 300 DPI)

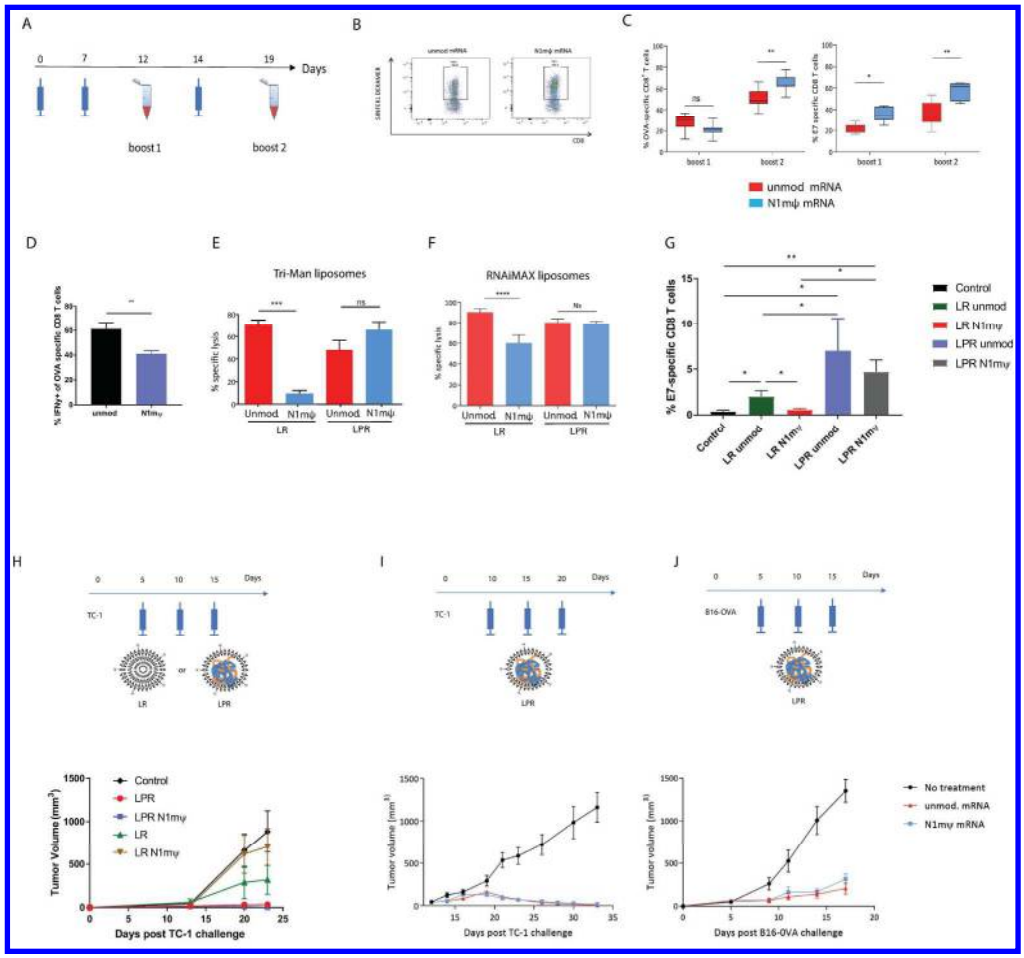

Figure 7. N1mψ nucleoside modified mRNA does not hamper antitumor T-cell immunity to LPR

195x182mm (300 x 300 DPI)

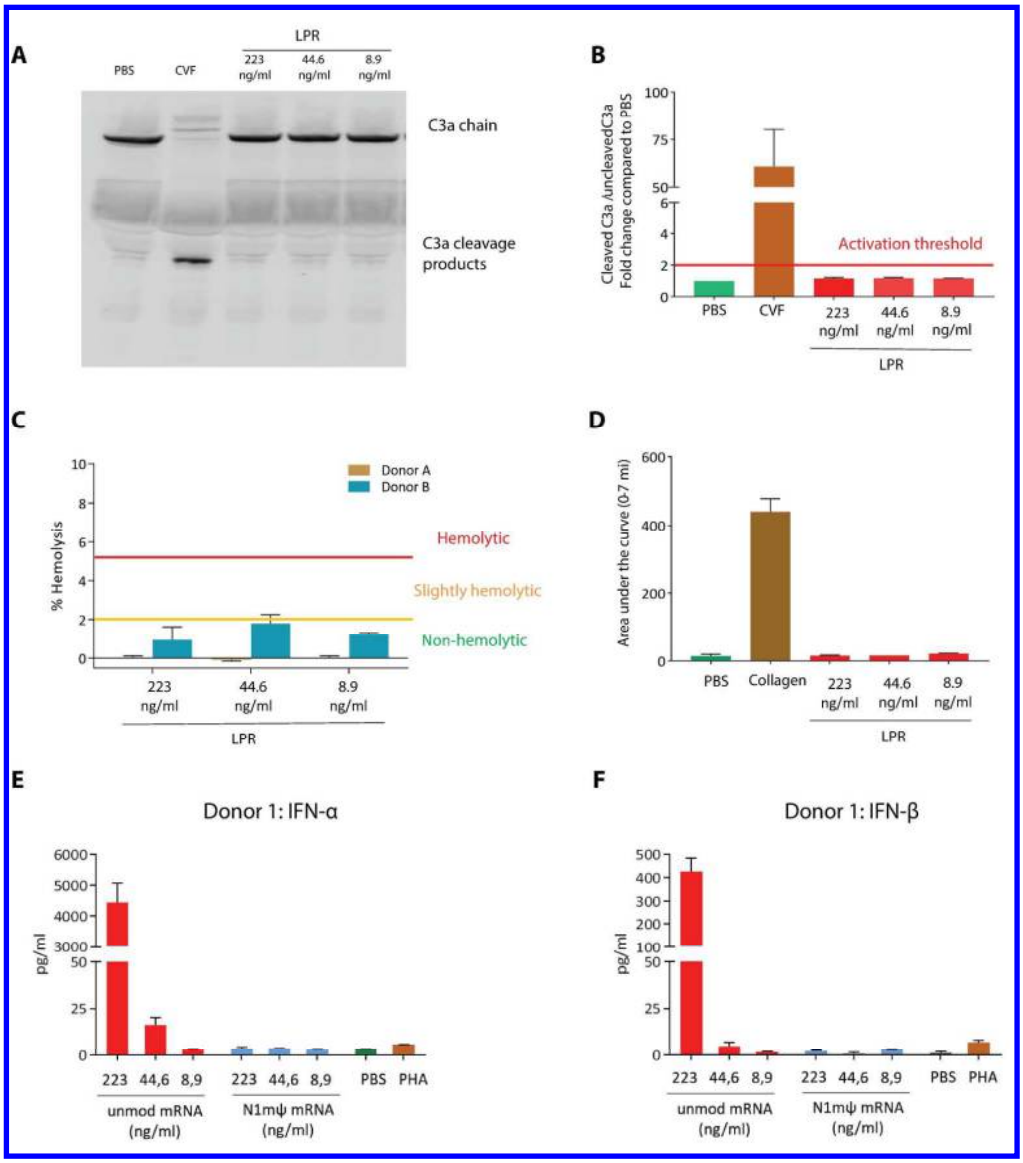

Figure 8. Characterization of LPR hemocompatibility on human blood

203x231mm (300 x 300 DPI)

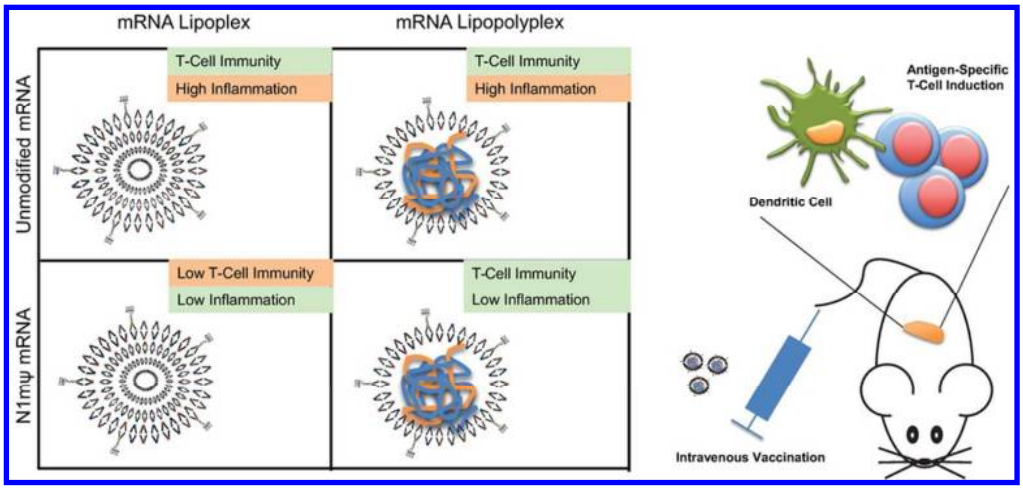

TOC

81x38mm (300 x 300 DPI)